ISTITUTO PER LA MATEMATICA APPLICATA
CONSIGLIO NAZIONALE DELLE RICERCHE
Via De Marini, 6
16149 Genova, Italia

AFFINE INVARIANT SKELETON OF 3D SHAPES[1]

M. Mortara, G. Patané

Technical Report N°. 12/2001

[1]Istituto per la Matematica Applicata, Consiglio Nazionale delle Ricerche, Genova, Italia.
email: {michela,patane}@ima.ge.cnr.it

1. Introduction

Shape description is the basis for recognition and is one of the key problems in similarity (matching) issues: the better is the description chosen for objects, the best (easier, more effective) the results will be. The ideal properties of a shape descriptor are that it naturally captures what we mean by shape in a concise but effective manner, and that it is automatically computable from the specification of an object by its boundary or its figure. Besides, a useful general-purpose description should necessarily satisfy the fundamental criteria of invariance, uniqueness and stability; a representation satisfying these conditions is suitable for tasks that call for recognition of noisy objects of arbitrary shape at arbitrary scale and orientation. Another likely property for a powerful shape descriptor is the capability of handling details, separating them from more essential shape characteristics; this can be achieved representing an object as a hierarchy of segments at successively smaller scales. This approach guarantees noise stability achieved by ignoring the lower levels of the hierarchy, and allows top-down operations on objects. Indeed is not a trivial problem to define a general shape descriptor which fulfils at the same time all these requirements, and often ad hoc solutions have been proposed depending on the application. For example a way of describing an object trough the configuration of its critical points with respect to a continuous function is the Reeb graph [13, 15] (see Figure 1(b)); when the high function is chosen, this is a very intuitive representation and it's useful for object compression, but it doesn't distinguish between structural and detail features, and besides is not affine-invariant too: it is dependent on the direction of the high function chosen, so that the same object can have completely different graphs according to its position in space. Another example of skeletal representation for planar shapes is the Medial Axis Transformation, defined by Blum in [3]; it's known that the Medial Axis is independent by the object position in space (it is affine- invariant), but unfortunately it is not stable in case of small perturbations. As underlined by Wyvill [17] a shape description independent of any coordinate system and able to distinguish between meaningful features and features details doesn't exist so far. He also pointed out which are the only tools we have to construct such a representation: the basic local characteristics of shape, i.e. surface normals, curvature and geodesic distance, together with the surface topology. We will show in the next sections our attempt to define an affine invariant skeletal representation following his advice.

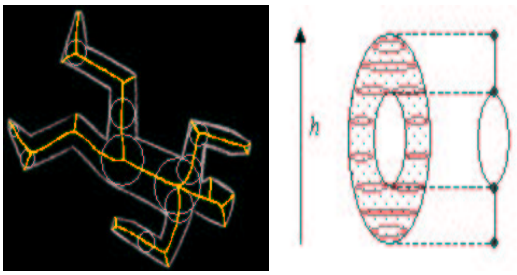

(a) (b)

Figure 1. (a) Medial Axis Transform, (b) Reeb graph with respect to the height function.

2. Review of related work

The aim of skeleton extraction is to take out and convert shape characteristics and properties of the surface into a compact representation. One of the best known shape descriptors

of this kind is the Medial Axis Transformation, defined by Blum in [3] for 2D shapes and extended to the 3D case by Sherbrooke [14]. In the planar case, the Medial axis of a shape is a graph defined as the locus of the centers of all the maximal discs contained inside the shape and having at least two points of contact with its boundary (see Figure 1(a)). It's known that this kind of representation is independent by the object position in space (invariance), but has the negative side that tiny perturbations of the boundary will produce extra edges in the graph, with no distinction between main and secondary features. Another method which is commonly used for shape description, and strictly related to our method, is the Reeb graph [1, 2, 13] whose definition is based on the Morse theory [11, 15]. First of all Morse theory states that the topology of a given manifold M can be studied analyzing the critical points of any smooth function $h : M \mapsto \mathbf{R}$ defined on the manifold. Typically, the map h represents the height function ($\forall p = (x, y, z) \in \mathbf{R}^3$, $h(x, y, z) = z$) whose critical points, i.e. peaks, pits and passes, are useful for shape description because they locate basic elements of shape description.

Starting from Morse theory, it is possible to define the Reeb graph [13] by coding the evolution of the "contours" on M defined by the function h as described by the following definition.

Definition. Let $h : M \mapsto \mathbf{R}$ be a real valued function on a compact manifold M. The *Reeb graph of M with respect to h* is the quotient space of $M \times \mathbf{R}$ defined by the equivalence relation $\sim$, given by $(p, h(p)) \sim (q, h(q))$, $p, q \in M$, if and only if

- $h(p) = h(q)$,
- p, q are in the same connected component of $h^{-1}(h(p))$.

Indeed, the Reeb graph is a 1-dimensional skeleton provided by a continuous scalar function on M which changes choosing different maps for the definition of $\sim$.

Even if different extensions of this theory [1, 2, 15] have been proposed, the Reeb graph suffers of at least two problems. Secondly, there is not distinction between large and small features due to the fact that the same connected components are collapsed into the same class without distinction of their sizes.

Because the height function h is not affine-invariant, in [9] a new map, based on the geodesic distance from a source point $p \in S$, has been defined to overcome this problem. The determination of p is not simple; the solution proposed by the authors is to define, for every $x \in S$, $h(x)$ as the sum of all geodesic distances $g(x, p)$ from x to p when p varies on the input manifold, that is,

$$h(x) := \int_{p \in S} g(x, p) dp.$$

This function is not invariant to scaling of the object and it is replaced by its normal representation defined as

$$\forall x \in S, \qquad h_n(x) := \frac{h(x) - \min_{x \in S}\{h(x)\}}{\max_{x \in S}\{h(x)\}}.$$

Another work on this topic [10] deals with the construction of centerlines from an unorganized collection of scattered data points lying on a tubular-shaped surface. First a neighbourhood graph of order n is computed for each point P in the set, connecting P to its n nearest points according to the Euclidean distance. A source point is chosen in the data set; the shortest paths on the neighbourhood graph between each point and the source point are computed and a new graph is obtained, together with a distance map coding the Euclidean length of all the shortest paths. Then k level set of the distance map are computed; the level sets are composed of points at a constant distance from the source. Finally, the

centerlines are constructed connecting the centroids of the corresponding connected components of successive levels. The resulting skeletal curves depends on the appropriate choice of the order of the neighbourhood graph, of the location of the source point and of the number k of the level sets in which to "slice" the surface. To choose the source point an heuristic is used which seems to work well on elongated tubular shapes such as blood vessels and bones, and examples are given to show that on these kind of input data the centerlines obtained with different source points are nearly the same. Anyway, the choice of only one source point determines a kind of privileged "slicing direction", fact that (together with a wrong choice of k) can lead to the loss of some features if the object is not strictly cylindrical (see Figure 2)

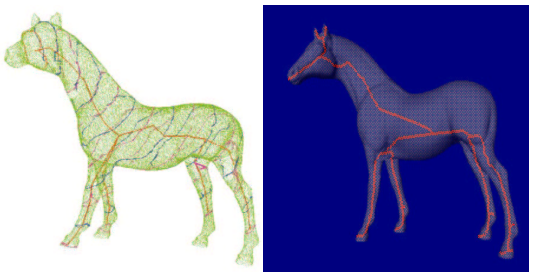

(a) (b)

FIGURE 2. (a) level sets and skeletal curves computed on the horse point set, as shown in [10], (b) result obtained with our algorithm.

3. Overview of the technique and contributions

The proposed construction of the skeleton of a 3D object represented by a triangular mesh is made in 4 steps.

(1) A curvature estimation is performed on the mesh and several zones of high curvature, which identify the surface features, are extracted (see Figure 3(a)). Since *curvature* is an intrinsic characteristic of the surface, a curvature based skeleton is coordinate independent. The procedure of curvature estimation is briefly discussed in section 4.
(2) Starting simultaneously from the centroid of the high curvature regions, topological rings consisting of vertices which has the same topological distance (minimum number of edges) from the nearest centroid are computed, growing of one edge at a time, until the all surface is covered (see Figure 3(b)).
(3) Then the graph is constructed. Each centroid of high curvature regions becomes the terminal nodes of the graph, while points of split or collision between topological rings during the expansion phase individuate the branching nodes. The centroid of the topological rings between two nodes are connected to form an edge (see Figure 3(c)). Steps 2 and 3 are described in detail in section 5. The mathematical definition of the graph as a quotient space is given in section 6, while its properties and a comparison with the Reeb graph is provided in section 7. Future work and results are presented in the last section.

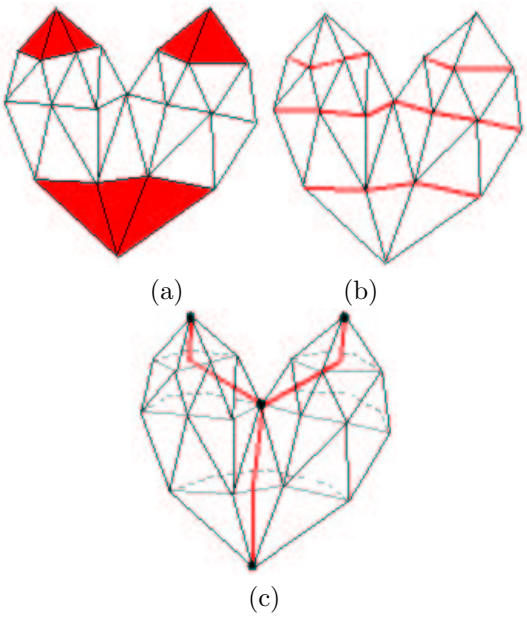

FIGURE 3. Main steps of the algorithm: (a) curvature evaluation, (b) topological expansion, (c) graph construction.

4. Curvature estimation on triangular meshes

The definition of the curvature at each point of a triangular mesh is not trivial because the last one is parameterized by a piecewise continuous function whose second derivatives are identically null. Among the different approaches which have been used to overcome the lack of a standard definition two main algorithms can be identified. The first one [8] ([16]) derives its discrete approximation at each vertex applying its continuous definition to a least-square paraboloid fitting its neighboring vertices (estimating its tensor curvature). The second one [4] is based on the Laplace-Beltrami operator and the Gauss map guaranteing the validity of differential properties such as area minimization and mean curvature flow [7].

In spite of the introduction of a multiresolution structure, all the previous approaches are usually sensitive to noise and small undulations requiring smoothness conditions on the input mesh. Furthermore, the smoothing process used to get stable and uniform curvature estimations introduces a deficiency in the magnitude evaluation and, consequently, difficulties in the accurate distinction between planar patches and curved surfaces with low curvature. Indeed, we need a classification of points which takes into account both curvature extrema and the related shape size in order to identify global features of maximal curvature which represent the input of our algorithm for shape abstraction.

The evaluation of the curvature of the surface at a point p [6], with respect to a level of detail R, is achieved calculating the normalized length $C := \frac{L}{2\pi R}$ of the intersection between the object surface S and the sphere of center p and radius R. Vertices having value C greater than a given threshold ($\pi/2$ in our implementation) are considered points of high-curvature. The connected components of adjacent points with high-curvature determine several regions on the mesh, which intuitively correspond to the protrusion of the object, and therefore identify the relevant features of the mesh. In this way, we are able to reduce the effect of noise, i.e. small geometric undulations, on the curvature estimation using a multiresolutive

approach with the use of a set of radii each one connected to the level of detail of the features which have to be considered relevant.

(a) (b)

FIGURE 4. Curvature estimation on the rabbit: red regions indicates high-curvature areas. In (b) a gaussian noise has been added to input points.

5. Graph construction

Any object can be seen as made essentially of a main body with several protrusions: for instance, the overall shape of a man consists of the torso from which head, arms and legs depart. From this point of view the main features of a 3D surface are its protrusions, and these are detectable by mean of curvature: at a protrusion extremity there must be a high curvature region. With reference to Figure 2, this is exactly what happens on the rabbit data set: the red regions identifying high curvature vertices are located on top of the ears, on the legs, on the muzzle and on the tail.

Following this considerations, we are going to construct the skeleton of a 3D surface as a curvature-based graph which, starting from high curvature regions, grows inside the shape towards the main body according to the mutual adjacency between features. First of all, for each high curvature region R_i a representative vertex p_i is selected (for a more pleasant visualization p_i is chosen as the centroid of R_i and computed as the farthest vertex from the region boundary; anyway we underline that from the topological point of view the arbitrary choice of p_i is irrelevant). The set of $\{p_i\}$ represent the terminal nodes of the graph; we will show in this section how the developed algorithm constructs the graph edges and determines the branching nodes according to a topological expansion method. First some considerations od mesh topology and definitions are given in the following section.

5.1. **Mesh topology.** We represent a triangular mesh S as the pair $S := \{V, F\}$ where $V := \{p_i = (x_i, y_i, z_i) : i = 1, \ldots, N\}$ is a list of N vertices and F is an *abstract simplicial complex* [5] which contains the adjacency information whose subsets come in three types: vertices $\{i\}$, edges $\{i, j\}$ and faces $\{i, j, k\}$. The topology in S is defined by F in the sense that we can construct the *1-neighborhood* structure as

$$\{N(i) : i = 1, \ldots, N\} \tag{1}$$

with

$$N(i) := \{j \in \{1, \ldots, N\} : (i, j) \in F\}.$$

The previous relation assigns each vertex i the set of its 1-neighborhood, that is, the vertices j such that (i,j) is an edge of the triangulation F. The size (radius) of the neighborhood structure can be recursively enlarged by defining a *n-neighborhood* as

$$
\begin{aligned}
&N(i_i,\ldots,i_k) := \textstyle\bigcup_{l=1}^{k} N(i_l),\\
&N^0(i) := \{i\},\\
&N^1(i) := N(i),\\
&N^n(i) := N^1(N^{n-1}(i)),\ n \geq 2.
\end{aligned}
\tag{2}
$$

Indeed, given a vertex $i \in \{1,\ldots,N\}$ we can define its *local neighborhood system* as

$$B_i := \{T(N^k(i)) : k = 0,\ldots\}$$

with

$$T(N^k(i)) := \bigcup_{l,p,q \in N^k(i), \{l,p,q\} \in F} T(l,p,q)$$

and $T(l,p,q)$ triangle with vertices l,p,q. Finally, we refer to the border of $T(N^k(i))$, i.e. $\partial T(N^k(i))$, as *topological ring of order k for i.*

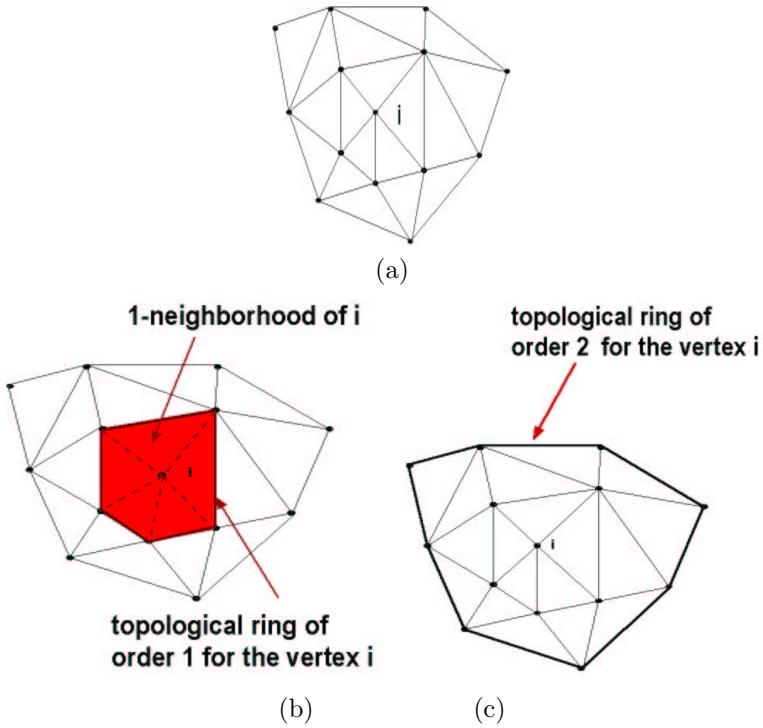

FIGURE 5. Local neighborhood system on a triangular mesh:(a) input mesh, (b),(c) topological rings of order 1,2 for i.

From the previous definitions the following conditions hold: $\forall i \in \{1,\ldots,N\}$

- $v_i \in T(N^k(i)), \qquad k = 0,\ldots$
- $T(N^k(i)) \subseteq T(N^{k+1}(i)), \qquad k = 0,\ldots$

- if S is connected, then

$$S = \bigcup_{k=1,\dots} T(N^k(i)).$$

5.2. **Topological expansion.** Above this point, we have segmented the mesh into significant/non significant regions, according to the curvature value at each vertex. Because high-curvature regions identify the extremities of the object protrusions, the skeleton of an object characterized in this way will have their representative points as terminal nodes. Indeed, for each region a representative vertex is chosen as the farthest, with respect to the topological distance, to the boundary. Starting from the representative vertices we can construct a skeleton of the object following a topological expansion approach, based on the idea of topological rings growing (expanding) from representative vertices and traversing the mesh, until rings split, collide with others, or can be expanded no more.

Starting at the same time from all the representative vertices, the topological rings expand one step at a time until:

- rings belonging to different representative vertices collide: a union occurs,
- a ring intersects itself: a split occurs,
- a ring can be expanded no more: the ring terminates.

Union. When expanding a topological ring we meet a vertex already belonging to the topological ring (of the same order) of another representative vertex the two rings intersects. From the point of view of the surface, this means that we have found a branching zone of the object where two distinct protrusions depart. In the same way, the corresponding skeleton will have a branch with two edges joining.

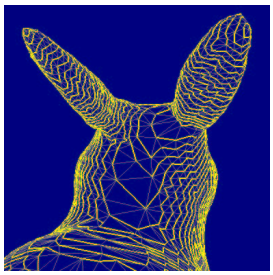

FIGURE 6. Example of union between rabbit ears.

The rings of each representative vertices, which determined the collision, can be expanded no more and the construction of their ring sets is completed. A new topological ring is created for the intersection vertex; in this case, unlike what happens for representative vertices, the first topological ring coded is the union of the two rings colliding.

Split. It can also happen that a ring intersects itself in one or more of its vertices; this is the situation of rings expanding near handles, through holes of the object or where a new protrusion starts. In this case, the intersecting ring splits in two parts and its expansion stops in favor of two new rings derived from the split. Like the union case, the adjacency between the father vertex and the two children is set.

Termination. After a finite number of steps, the splitting and joining rings will cover the whole surface. A ring terminates when the next step would produce a non valid boundary, that is, with less than 3 vertices. When a ring terminates, it means that there were no more

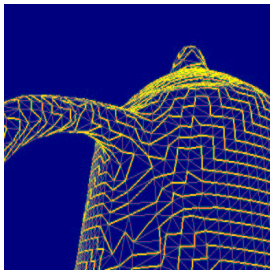

FIGURE 7. Example of split on the handle of the pot.

significant features in the object. Indeed, branches of the skeleton will be not produced in the case of a ring which terminates without having a union or a split.

5.3. **Graph visualization.** When all the ring sets of the representative vertices and the ones created during their expansion are terminated, the algorithm can draw the skeleton as the adjacency graph encoded during the expansion phase:

- each representative vertex gives a *terminal node*,
- each intersection vertex (occurring in a union or a split configuration) gives a *branching node*,
- the topological rings, belonging to the ring set of a node, gives an arc which goes out from that node [2]. In particular, an arc is drawn joining the center of mass of all its topological rings.

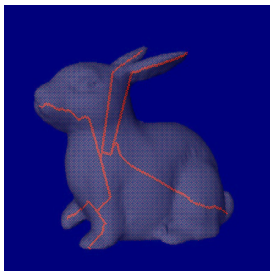

FIGURE 8. Example of skeleton on the rabbit.

6. Graph as quotient space

In this section we are concerned with the formulation of the graph construction for triangular meshes and manifolds demonstrating that it is the quotient space of the input object surface S with respect to an equivalence relation $\sim$. The proposed construction of G as $S/\sim$ enables to:

- verify that G depends only on the topology of S and on a finite set of representative points $\{p_1, \ldots, p_n\}$ in S of high-curvature values,
- verify that G is affine-invariant; this characteristic represents one of the main properties of G and of this theory not shared by other approaches,

[2]Note that when a split or a union occurs, there can be two arcs going off the same node: in this case two distinct ring sets are created for the same node. So each ring set always defines one node and one arc.

- extract the information on G (e.g. compactness, connectivity, etc.) starting from S and exploiting the properties of the quotient space.

6.1. **Graph definition for triangular meshes.** Selected a point p_i in S we introduce the function

$$\begin{aligned} f_{p_i} : S &\mapsto \mathbf{N} \\ x &\mapsto f_{p_i}(x) := \min\{k : x \in T(N^k(i))\} \end{aligned}$$

,i.e., $f_{p_i}(x)$ is the minimal *topological distance* between p_i and x.

We can extend in a simple way the previous function to a finite set of vertices $\{p_1, \ldots, p_n\}$ as

$$\begin{aligned} f : S &\mapsto \mathbf{N} \\ x &\mapsto f(x) := \min_{k=1,\ldots,n}\{f_{p_k}(x)\} \end{aligned}$$

, i.e., f assigns to x its minimal topological distance with respect to the case of more than one vertex ($n = 1, f = f_{n_1}$).

Starting from f and S we are able to construct the relation $\sim$ as follows:

$$p, q \in S, \;\; p \sim q \;\text{ iff }\; f^{-1}(f(p)) \cap f^{-1}(f(q)) \neq \emptyset. \tag{3}$$

First of all, (3) implies that if $f(p) \neq f(q)$ then $p \not\sim q$; in fact, we have

$$f^{-1}(f(p)) \cap f^{-1}(f(q)) = f^{-1}(f(p) \cap f(q)) = f^{-1}(\emptyset) = \emptyset.$$

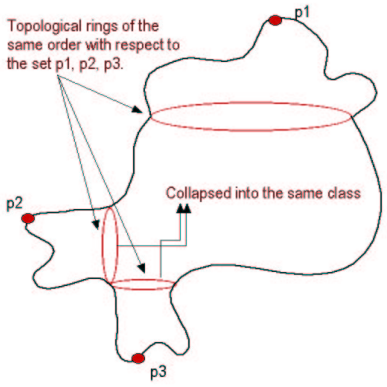

FIGURE 9. Example of topological rings on a manifold.

In other words, necessary condition for $p \sim q$ is that $f(p) = f(q)$, that is, p and q have the same topological distance from the selected set of vertices $\{p_1, \ldots, p_n\}$. Secondly, two points p and q are in relation with respect to $\sim$ if and only if they have non-disjoint topological rings (i.e. $f^{-1}(f(p)) \cap f^{-1}(f(q)) \neq \emptyset$) of the same order (i.e. $f(p) = f(q)$).

Now we want to investigate the properties of $\sim$:

- reflexive: $\forall p \in S, p \sim p$,
- symmetric: $\forall p, q \in S, p \sim q \Rightarrow q \sim p$,
- transitive: $\forall p, q, r \in S, p \sim q, q \sim r \not\Rightarrow p \sim r$. In fact, the intersection of sets is not transitive on $P(X) := \{X : X \subseteq S\}$.

From the previous relations it follows that

$$G = S/\sim = \{[x] : x \in S\}$$

where the class of x is represented by the set

$$[x] := \{y \in S : y \sim x\}.$$

Furthermore, the following conditions hold:

- $[x] \neq \emptyset, \forall x \in S$ (i.e. every class is not empty),
- $x \sim y \Rightarrow [x] \cap [y] = \emptyset$ (i.e. two vertices which satisfy the relation $\sim$ have non-empty intersection. Generally, the inverse condition is not true because $\sim$ is not transitive),
- $\bigcup_{x \in S}[x] = S$ (i.e. $\{[x]\}_{x \in S}$ represents a cover of S).

6.2. **Graph definition for manifolds.** We want to extend the previous model to a compact manifold without boundary embedded in $\mathbf{R}^3$ with the Euclidean topology underlining the general application of our model for the extraction of an affine-invariant shape description. In the following we review definitions and concepts on topology introducing the basic notions and referring to [5] for further readings. The structure of the section reflects that of the previous one facilitating the parallelism between the continuous case study and the discrete one which has been used for the implementation of the algorithm.

Introduced a topological space (X, τ), we define as

- *induced topology of X in $S \subseteq X$*: the topology τ_S defined as

$$\tau_S := \{A \cap S : A \in \tau\},$$

- *local base of p in X*: the family B_p consisting of neighborhoods of the point p such that for every neighborhood U of p there is a set $V \in B_p$ such that $V \subseteq U$,
- *boundary of $A \subseteq X$*: $\partial A := \overline{A} \cap \overline{X - A}$, that is, the intersection between the closure of the set A and its complement $(X - A)$ in X.

Given a point $p \in S$ we define, for every $R > 0$, the open ball of center p and radius R as

$$B(p, R) := \{x \in \mathbf{R}^3 : \|x - p\|_2 < R\}$$

and with $U(p, R)$ the connected component of p in $S \cap B(p, R)$. Indeed, we can associate to each point $p \in S$ the family of neighborhoods $\{U(p, R)\}_{R>0}$, with $U(p, 0) := \{p\}$, centered in p. From the previous relations we can derive the following properties which will be used for constructing the graph of S:

- $\{U(p, R)\}_{R>0}$ is a local base of the space S at the point p with respect to the topology τ_S induced by the Euclidean topology τ in S. This property follows using the definition of τ_S and the fact that the set $\{B(p, R)\}_{R>0}$ is a local base of p in $(\mathbf{R}^3, \tau)$.
- $R_1 < R_2 \Rightarrow U(p, R_1) \subseteq U(p, R_2)$: in fact, $R_1 < R_2 \Rightarrow B(p, R_1) \subseteq B(p, R_2) \Rightarrow S \cap B(p, R_1) \subseteq S \cap B(p, R_2) \Rightarrow$ the connected component of p in $S \cap B(p, R_1)$ is a subset of that in $S \cap B(p, R_2)$.

Introduced the counterparts of the concepts defined for the triangular mesh, we can extend the previous functions as described in the following. Chosen a point $p \in S$, we define the map

$$\begin{aligned} f_p : \mathbf{R}^3 &\mapsto \mathbf{R} \\ x &\mapsto f_p(x) := \|p - x\|_2 \end{aligned}$$

and then, fixed a set of points $P := \{p_1, \ldots, p_n\} \subseteq S$, we construct its extension to the set P as

$$\begin{aligned} f : S &\mapsto \mathbf{R} \\ x &\mapsto f(x) := \min_{k=1,\ldots,n}\{f_{p_k}(x)\}. \end{aligned}$$

The function f is continuous because it is the composition of the continuous maps

$$(f_{p_1}, \ldots, f_{p_n}) : S \mapsto \mathbf{R}^n$$
$$x \mapsto (f_{p_1}(x), \ldots, f_{p_n}(x))$$

and

$$\min : \mathbf{R}^n \mapsto \mathbf{R}$$
$$(x_1, \ldots, x_n) \mapsto \min_{i=1,\ldots,n}\{x_i\}.$$

Indeed, in analogy with the previous section, we can introduce the relation $\sim$ as: $p, q \in S$ $p \sim q$ if and only if we can choose $R > 0$ such that $f(p) = f(q)$ and p, q belong to the same connected component of $f^{-1}(f(p))$. In other words, necessary and sufficient condition for $p \sim q$ is that p and q have the same topological distance from the selected set of points $\{p_1, \ldots, p_n\}$ and they belong to the connected component of the pre-image of their (common) value $f(p)$. The relation $\sim$ is symmetric, reflexive and transitive because it is the intersection of two equivalence relations (i.e. function equality and membership to the same connected component). Using the properties of the quotient space, we deduce that $\sim$ induces in S a decomposition into a family of non-empty, disjoint topological classes.

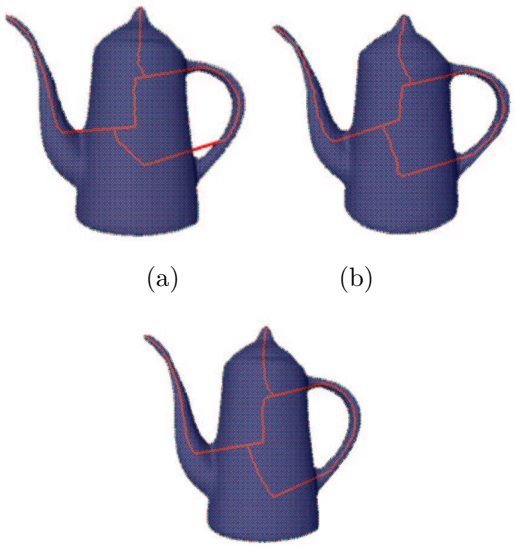

(a) (b)

(c)

FIGURE 10. (a) Skeleton on the original data set, (b) Skeleton on the regularized mesh, (c) Skeleton on the refined mesh.

If the input surface S is compact/connected then G is compact/connected; anyway, the canonical projection

$$\pi : S \mapsto G = S/\sim$$
$$x \mapsto [x]$$

is continuous with respect to the quotient space topology (i.e. $A \subseteq G$ is open if $\pi^{-1}(A)$ is open in (S, τ)).

Remark. The previous construction can be reduced to define the function f such that $Im(f) := \{f(x) : x \in S\} \subseteq \mathbf{N}$ choosing, for a given point $p \in S$, its local base as

$B_p = \{S \cap B(p, kn)\}_{n \in \mathbf{N}}$, with $k \in \mathbf{R}^+$ step, and defining for every $x \in S$ $f(x) := \min_{k=1,\ldots,n}\{f_{p_k}(x)\}$ where $f_{p_i}(x) := \min\{n : x \in B(p_i, kn)\}$.

7. Properties and comparison

In this section we want to present the main properties and distinctions of the graph G with respect to other approaches as the Reeb graph. This comparison is evaluated considering the topological properties of both graphs, as quotient spaces, and a set of experimental results which underline the main drawbacks of the previous theory for shape abstraction.

The complexity of the proposed graph, in terms of number of nodes and branches, depends on the shape of the input object and of the number of points $\{p_i\}_{i=1}^n$ which we have selected using the curvature estimation criterion. The construction of G is guided, in the first step, by the topology of the mesh through the connectivity relations in F and, secondly, by the geometry V which influences the chosen representative point p for its equivalence class $[p]$. The only requirement for an optimal construction of the graph deals with a uniform mesh finalized at having a topological distance between points to which corresponds a medium step on the mesh (see Figure 7).

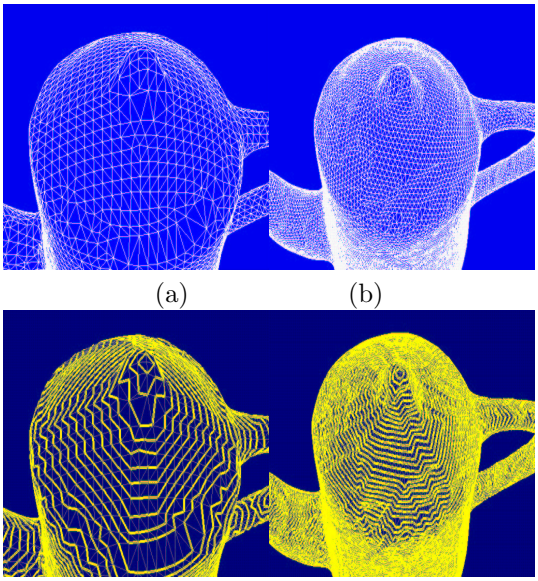

Figure 11. (a) Input mesh, (b) refined mesh, (c) topological rings on (a), (d) topological ring on (b).

The graph structure is not incremental in the sense that if we add a point p_{n+1} to the set $\{p_1, \ldots, p_n\}$, which is used for the construction of G, the new graph $\tilde{G}$ defined by $\{p_1, \ldots, p_n, p_{n+1}\}$ is not achieved adding to G the new branch starting from p_{n+1}.

Our graph is affine-invariant (translation, rotation, scaling and shear) because the function f which has been used for defining the relation $\sim$ and the quotient space G does not rely on a local system of coordinates in which the object surface is embedded as it happens in the case of the Reeb graph constructed, for example, using the height function. However, we want to stress that both graphs are build in the same way choosing only two different functions. More precisely, our graph (the Reeb graph) codes the surface shape by analyzing

the evolution of topological arcs (contours) obtained by the mesh topology (intersecting the surface with a family of planes along a chosen direction). An interesting question is: does a relation between them exist? In other words, which hypothesis on S ensure that the related quotient spaces are homeomorphic? Finally, the continuous definition of the graph can be used in a simple way to extend its construction to a polyhedral surface introducing the topological structure as done for the triangular mesh analysis.

8. Conclusions and future works

The starting point of this work is represented by previous approaches on shape abstraction attempting to propose possible extensions of the Reeb graph which represents the core of our model.

The graph presented in this paper represents the first step toward the construction of a complete framework for shape abstraction, analysis and comparison. One of the most involving application that we foresee and we want to approach is shape matching. The affine-invariant structure of this graph and its description as quotient space enable to convert the matching problem between two graphs G and H into a multiple framework whose solution is achieved defining a matching function which is an homeomorphism between G and H plus a penalty function which takes into account the geometry of the objects associated to them.

References

[1] M. Attene, S. Biasotti and M. Spagnuolo, "Re-meshing Techniques for Topological Analysis", in *Proceeding of Shape Modeling International 2001*, IEEE Press, Genoa, May 2001, pp.142-151.

[2] S. Biasotti, B. Falcidieno and M. Spagnuolo, "Extended Reeb Graphs for Surface Understanding and Description", in *Proceedings of the* 9^{th} *Discrete Geometry for Computer Imagery Conference, LCNS*, Springer Verlag, Uppsala, 2000.

[3] H. A. Blum, "Transformation for Extracting New Descriptors of Shape", *Models for Perception of Speech and Visual Form*, MIT Press 1967, 362-381.

[4] M. Desbrun, M. Meyer, P. Schroeder, A.H. Barr, "Discrete Differential-Geometry Operators in nD", July 22, 2000. URL: http://www.multires.caltech.edu/pubs/pubs.htm

[5] R. Engelking and K. Sielucki, *Topology: a geometric approach*, Sigma Series in Pure Mathematics, Volume 4, Heldermann Verlag, Berlin, 1992.

[6] B. Falcidieno, M. Mortara, G. Patané, J. Rossignac, M. Spagnuolo, *Tailor: understanding 3D shapes using curvature*, Technical Report N.??/2001, Istituto per la Matematica Applicata, Consiglio Nazionale delle Ricerche.

[7] V. Guillemin, and A. Pollack, *Differential Topology*, Englewood Cliffs, NJ: Prentice-Hall, 1974.

[8] B. Hamman, "Curvature Approximation for Triangulated Surfaces", *Computing Suppl.* 8, 1993, pp. 139-153.

[9] M. Hilaga, Y. Shinagawa, T. Kohmura, T.L. Kunii, "Topology Matching for Fully Automatic Similarity Estimation of 3D Shapes", in *Computer&Graphics, Proceeding of Siggraph 2001*, Los Angeles, 2001.

[10] F. Lazarus, A. Verroust, "Extracting skeletal curves from 3D scattered data", in *The Visual Computer*, vol. 16, N. 1, pp 15-25, 2000.

[11] J. Milnor, *Morse Theory*, Princeton University Press, New Jersey, 1963.

[12] M. Mortara and M. Spagnolo, *Hierarchical Representation of 2D Polygons based on Approximate Skeletons*, Technical Report N. 8/2000, Istituto per la Matematica Applicata, Consiglio Nazionale delle Ricerche.

[13] G. Reeb, "Sur les points singuliers d'une forme de Pfaff completement integrable ou d'une fonction numerique", *Comptes Rendus Acad. Sciences*, Paris, 1946, 222:847-849.

[14] E. C. Sherbrooke, N. M. Patrikalakis and E. Brisson, "An Algorithm for the Medial Axis Transform of 3D Polyhedral Solids", *IEEE Transaction on Visualization and Computer Graphics*, Vol. 2, N.1, March 1996.

[15] Y. Shinagawa, T.L. Kunii, and Y.L. Kergosien, "Surface Coding Based on Morse Theory", *IEEE Computer Graphics & Applications*, 1991, pp. 66-78.

[16] G. Taubin, "Estimating the Tensor Curvature of a Surface from a Polyhedral Approximation", *Fifth International Conference on Computer Vision (ICCV'95).*

[17] G. Wyvill and C. Handley, "The 'Thermodynamics' of Shape", *Proceedings of Shape Modeling International 2001*, IEEE Press, Genova, Italy, May 2001, 2-8.